RSC Advances

PAPER

View Article Online
View Journal | View Issue

Cite this: *RSC Adv.*, 2022, **12**, 25912

Therapeutic deep eutectic solvent-based microemulsion enhances anti-inflammatory efficacy of curcuminoids and aromatic-turmerone extracted from *Curcuma longa* L.†

Nassareen Supaweera, [a] Wanatsanan Chulrik, [b] Chutima Jansakun, [b] Phuangthip Bhoopong, [bd] Gorawit Yusakul *[c] and Warangkana Chunglok *[bd]

To diminish chemical waste and improve the delivery of *Curcuma longa* L. (CL) constituents, microemulsions based on hydrophobic deep eutectic solvents (HDESs) were designed as ready-to-use solvents for CL extraction. The microemulsion (ME) of the ME-23 formulation (HDES/Tween 80 : propylene glycol (1 : 1)/water, 25/70/5) displayed CL extraction yields of 1.69, 3.04, 7.36, and 1.39 wt% of bisdemethoxycurcumin, demethoxycurcumin, curcumin, and aromatic-turmerone, respectively. The ME-23 without CL chemical constituents and ME-23-based CL extract inhibited NO production with an IC_{50} value of 0.0136 ± 0.0023%v/v and a curcumin IC_{50} value of 75.2 ± 6.7 nM, respectively, and simultaneously lowered inflammatory cytokines tumor necrosis factor-α, interleukin (IL)-6, and IL-1β production in lipopolysaccharide-activated murine macrophages. Authentic curcumin in ME-23 possessed superior NO inhibitory activity, which was 103-fold more effective than curcumin prepared in the conventional solvent dimethyl sulfoxide. ME-23 was also capable of delivering curcumin into murine macrophages. After 30 days of storage in HDES and HDES-based ME, curcumin remained more than 90%. ME-23 provides advantages for CL extraction, constituent delivery, and anti-inflammatory functions that can be applied to pharmaceutical and cosmetic products.

Received 13th June 2022
Accepted 3rd September 2022

DOI: 10.1039/d2ra03656h

rsc.li/rsc-advances

Introduction

Turmeric or *Curcuma longa* L. (CL) and its principal constituent curcuminoids (Curs) are attracting global attention as ingredients in health products with a wide range of health benefits.[1] Imports of CL to Europe, from 2019 to 2020, rose by 13% in total value, totaling more than €64 million.[2] The absorption and stability of curcuminoids are the primary obstacles to the development of CL-related products. The production of organic solvent waste also hinders the extraction of CL because the chemical constituents of CL are not soluble in water.

Curs are orange-yellow lipophilic chemicals found in the CL rhizomes. They primarily constitute curcumin (Cur, 77%), demethoxycurcumin (Dem, 17%), and bisdemethoxycurcumin (Bis, 3%).[3] Owing to their biological activities against inflammatory pathways, turmeric extracts and Cur are useful in treating chronic inflammatory diseases.[4] The Cur metabolites tetrahydrocurcumin and hexahydrocurcumin have been shown to exhibit potent anti-inflammatory activity in various *in vitro* and *in vivo* studies.[5,6] Meta-analyses reveal that Curs provide superior pain relief compared to non-steroidal anti-inflammatory drugs (NSAIDs) for osteoarthritis, and Curs have fewer side effects.[7] Additionally, nano-Cur (low dose) has been linked to a significant reduction in fasting blood glucose and an improvement in dyslipidemia.[8] Cur and its derivatives have a wide variety of therapeutic applications.

Inflammation is a fundamental biological process triggered by the response of the immune system to stimuli.[9] Macrophages are innate immune system effector cells that recognise pathogens through their toll-like receptors (TLRs) and initiate an inflammatory response.[10] Lipopolysaccharide (LPS), a Gram-negative bacterial endotoxin, binds to the TLR4 receptor on the macrophage cell membrane, leading to the induction of intracellular signaling cascades and inflammatory response.[11] Inducible nitric oxide synthase/nitric oxide (NO),

[a]*Health Sciences (International Program), College of Graduate Studies, Walailak University, Nakhon Si Thammarat, 80160, Thailand. E-mail: cwarang@wu.ac.th; aon.cwarang@gmail.com*

[b]*School of Allied Health Sciences, Walailak University, Nakhon Si Thammarat, 80160, Thailand*

[c]*School of Pharmacy, Walailak University, Nakhon Si Thammarat, 80160, Thailand. E-mail: gorawit.yu@wu.ac.th; gorawit.yu@mail.wu.ac.th*

[d]*Food Technology and Innovation Research Center of Excellence, Research and Innovation Institute of Excellence, Walailak University, Nakhon Si Thammarat, 80160, Thailand*

† Electronic supplementary information (ESI) available. See https://doi.org/10.1039/d2ra03656h

cyclooxygenase-2/prostaglandin E_2, and inflammatory cytokines, such as tumor necrosis factor-α (TNF-α), interleukin (IL)-6, and IL-1β, are among the common key mediators of inflammation.[12] Curs target these inflammatory mediators in the modulation of inflammation and immune processes.[13]

However, owing to its insoluble nature and rapid metabolism, Cur is poorly absorbed in the gastrointestinal tract, resulting in low bioavailability and inconsistent clinical outcomes and necessitating the use of high doses. Therefore, various delivery systems have been developed for Cur and Curs. Cur bioavailability was 22.6-fold greater in microemulsions (MEs) than in suspensions.[14] In a rat model, Cur loaded in long-PEGylated solid lipid nanoparticles increased bioavailability by >12.0-fold compared to Cur solution.[15] Micelle formulation of Cur is 277-, 114-, and 185-fold more bioavailable than native Cur in women, men, and all subjects, respectively.[16] The first step in ensuring sustainable growth of the turmeric industry is to develop simple and environmentally friendly methods for producing readily absorbable Curs for anti-inflammatory applications.

Deep eutectic solvents (DESs) can enhance the solubility, permeation, and absorption of active pharmaceutical ingredients.[17] When a component of DESs can act as a therapeutic agent, it is referred to as therapeutic deep eutectic solvents (THEDES).[18] Menthol is known to have gastroprotective properties through anti-apoptotic, antioxidant, and anti-inflammatory mechanisms.[19] Menthol has also been used to enhance the permeation of medicines.[20] Octanoic acid (OA) inhibited the transcription of the *IL-8* gene in Caco-2 cells[21] and attenuated the inflammatory response by suppressing both mRNA and protein expression of TLR4, nuclear factor-kappa B, and TNF-α in LPS-activated RAW264.7 cells.[22]

When hydrophobic DESs (HDESs) containing OA and menthol are used as the oil phase in ME systems, HDES-based ME is hypothesised to enhance the anti-inflammatory effects by facilitating the delivery of HDES component Curs and aromatic (*ar*)-turmerone (*ar*-Tur) from the CL extract. Therefore, this study aimed to compare the physical characteristics, extraction capacity, and anti-inflammatory activity of various HDES-based MEs and their CL extracts in LPS-activated RAW264.7 macrophages. The bioactive HDES-based ME can be further optimised as environmentally friendly extraction processes and formulated as drug delivery systems to enhance the bioavailability of Curs and *ar*-Tur.

Results and discussion

Characteristics of deep eutectic solvent-based microemulsions

Microemulsions are typically used to provide drugs with low solubility as they enhance absorption. HDES-based ME formulations may help disperse Curs and *ar*-Tur in medicinal formulations. Specific components created the ME when the oil phase of the MEs was OA : menthol (70 : 30, 40 : 60, and 20 : 80 mass ratio), and the surfactant mixture was Tween 80 : propylene glycol (PG) (1 : 1), as shown in the pseudo-ternary phase diagram (Fig. 1). In this study, the water content of the ME was fixed at 5%. MEs formulated with HDES of OA : menthol (70 : 30 and 40 : 60) were classified as an oil-in-water emulsion (o/w) when the HDES concentration was

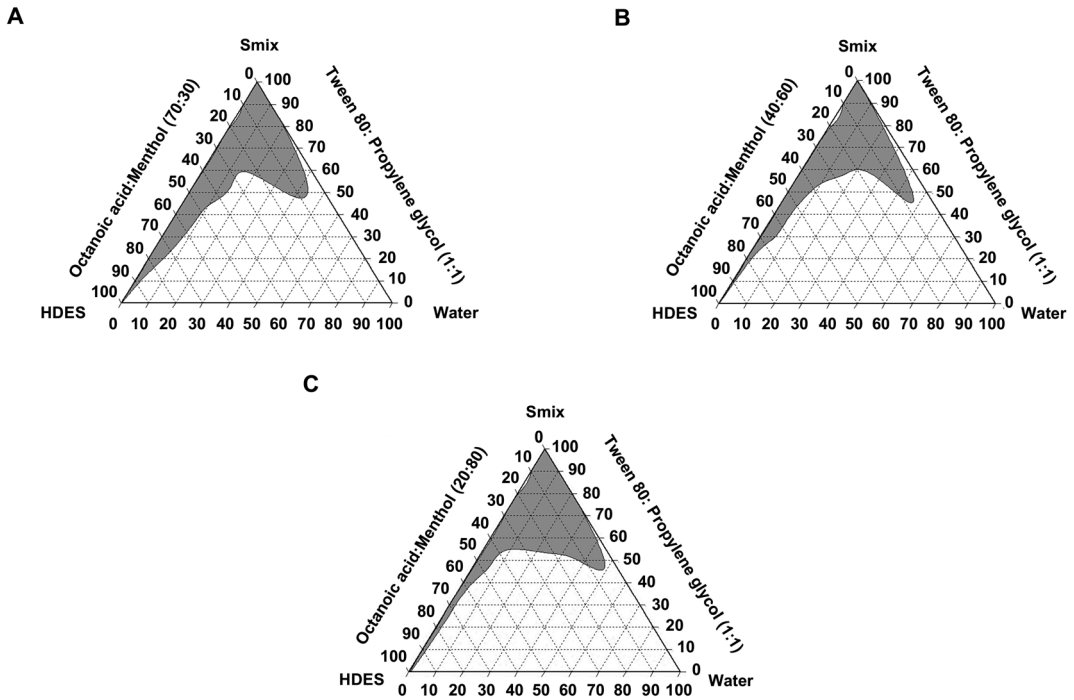

Fig. 1 Pseudo-ternary phase diagrams of HDESs, OA : menthol at 70 : 30 (A), 40 : 60 (B), and 20 : 80 (C), in which gray represents the microemulsion existence range. Tween 80 : propylene glycol (PG) was used as a surfactant mixture (Smix).

Table 1 Components and characteristics of HDES-in-water microemulsions and *C. longa* extracts ($n = 3$, mean ± SEM)

	Components (wt%)			Blank microemulsion			Microemulsion-based extracts			
Microemulsion	HDES	Smix	Water	Size (nm)	PDI	Zeta potential (mV)	Size (nm)	PDI	Zeta potential (mV)	Type of microemulsion
HDES of octanoic acid : menthol (70 : 30, mass ratio)										
ME-71	5	90	5	8.05 ± 0.87	0.49 ± 0.02	−45.3	8.48 ± 0.26	0.58 ± 0.02	−58.4	o/w
ME-72	15	80	5	8.71 ± 1.20	1.0 ± 0.0	−17.1	4.13 ± 0.30	0.75 ± 0.06	−63.3	o/w
ME-73	25	70	5	28.1 ± 5.5	1.0 ± 0.0	−54.4	12.2 ± 1.85	0.89 ± 0.05	−45.2	o/w
ME-74	35	60	5	6.58 ± 0.78	0.61 ± 0.04	−59.9	9.20 ± 0.18	0.83 ± 0.03	−50.4	o/w
ME-75	45	50	5	28.3 ± 1.3	0.88 ± 0.12	−21.8	11.3 ± 0.64	0.37 ± 0.10	−10.7	w/o
ME-76	55	40	5	6.25 ± 0.11	1.0 ± 0.0	−60.7	123 ± 13	0.61 ± 0.03	−72.6	w/o
ME-77	65	30	5	57.2 ± 6.4	0.99 ± 0.01	−27.3	128 ± 10	0.22 ± 0.06	−89.6	w/o
ME-78	75	20	5	60.6 ± 5.5	0.99 ± 0.01	−5.75	140 ± 4	0.58 ± 0.16	−39.0	w/o
HDES of octanoic acid : menthol (40 : 60, mass ratio)										
ME-41	5	90	5	5.95 ± 0.50	0.54 ± 0.02	−65.2	9.48 ± 0.19	0.77 ± 0.02	−7.45	o/w
ME-42	15	80	5	7.21 ± 0.53	0.94 ± 0.06	−65.9	14.4 ± 1.32	0.96 ± 0.04	−34.7	o/w
ME-43	25	70	5	23.1 ± 1.4	0.98 ± 0.00	−42.8	55.5 ± 4.14	0.69 ± 0.07	−3.09	o/w
ME-44	35	60	5	15.1 ± 2.4	1.0 ± 0.0	−6.40	265 ± 30	0.46 ± 0.15	−11.3	o/w
ME-45	45	50	5	25.2 ± 2.0	1.0 ± 0.0	−22.1	34.4 ± 3.2	0.94 ± 0.04	−39.3	w/o
ME-46	55	40	5	20.8 ± 1.7	0.91 ± 0.08	−48.0	227 ± 8	0.89 ± 0.07	−97.4	w/o
ME-47	65	30	5	41.1 ± 3.6	1.0 ± 0.0	−76.9	16.9 ± 0.9	0.26 ± 0.07	−21.8	w/o
HDES of octanoic acid : menthol (20 : 80, mass ratio)										
ME-21	5	90	5	7.13 ± 1.22	0.64 ± 0.02	−45.1	10.3 ± 0.4	0.79 ± 0.11	−4.40	o/w
ME-22	15	80	5	7.45 ± 0.30	0.60 ± 0.04	−42.0	10.2 ± 0.1	0.87 ± 0.07	−45.5	o/w
ME-23	25	70	5	15.9 ± 1.9	0.73 ± 0.06	−15.0	99.1 ± 2.3	0.89 ± 0.04	−38.0	o/w
ME-24	35	60	5	38.1 ± 5.5	0.44 ± 0.07	−2.40	34.0 ± 1.8	0.76 ± 0.08	−27.5	o/w
ME-25	45	50	5	11.1 ± 1.0	0.82 ± 0.06	−33.6	248 ± 7	0.94 ± 0.04	−18.8	o/w

between 5% and 35% (Table 1). However, the ME was water-in-oil emulsion (w/o) when the HDES content was greater than or equal to 45%. Using an octanoic acid : menthol mass ratio of 20 : 80 as the oil phase, o/w MEs (ME-21 – ME-25) were produced. Ethyl oleate, oleic acid, corn oil, soybean oil, Labrafac CC, and other oils are employed as oil phases of ME.[23] According to our findings, HDES is useful as an oil phase in microemulsions. Only o/w MEs were further examined for anti-inflammatory properties.

Blank microemulsions with a size between 5.95 and 60.6 nm are classed as MEs (<100 nm) according to Table 1. With ME-71 – ME-75, ME-41 – ME-43, ME-45, ME-47, and ME-21 – ME-24, the microemulsion-based CL extract sizes were still less than 100 nm (Table 1). Therefore, some MEs based on HDES can be loaded with CL constituents, and their size is still within an acceptable range. The size of several HDES-based ME formulations in our study was appropriate at less than 20 nm and remained small after being loaded with CL extract. The optimised self-microemulsifying drug delivery systems (SMEDDS) for Cur formulations contained 70% surfactant mixes of Cremophor EL and Labrasol (1 : 1) and 30% oil mixtures of Labrafac PG and Capryol 90 (1 : 1), and yielded ME size ranges of 25.8–32.8 nm.[23] Another study found that the optimal formulation of ME consisting of Capryol 90 (oil phase) and a mixture of Cremophor RH40 : Transcutol P as a surfactant produced a particle size of 26.1–29.8 nm.[14]

The polydispersity index (PDI) of HDES-based MEs and their extracts is high, with PDI values more than 0.7, indicating that the sample has a very broad particle size distribution.[24] The appropriate ME components and Cur loading should be further optimised to improve their uniform particle size. When the selected HDES-based MEs and their CL extracts were diluted in water (1 : 1000), the size of the ME remained small (≤51.3 nm), and the PDI of most MEs was 0.3–0.7 (Table S1†). These results demonstrate that the sizes of the ME and PDI are suitable when they are prepared for cell-based experiments. The HDES-based ME may have a bimodal impact, with the HDES increasing solubility and menthol improving permeability[20] as well as a function of the ME structure promoting cell entry.[14,23,25] Therefore, the HDES-based ME may be superior to the conventional ME. The additional comparison between HDES-based ME and conventional ME should be further investigated for Cur delivery and anti-inflammatory activity.

Extraction yields of deep eutectic solvent-based microemulsions

The ME-43 formulation produced the highest extraction yields for Bis, Dem, Cur, and *ar*-Tur (2.04, 3.80, 9.07, and 1.66 wt%, respectively) when HDES-based MEs were used as extraction solvents (Table 2). The largest yields of Cur were produced with ME-74, ME-43, and ME-25 compared to MEs of each HDES. The ME-74 formulation produced extraction yields for Bis, Dem, Cur, and *ar*-Tur (1.32, 2.56, 6.15, and 1.11 wt%, respectively), while those compounds were obtained at 1.90, 4.16, 8.10, and 1.50 wt% by ME-25. Based on all MEs, the correlated extraction yields of Cur and *ar*-Tur were determined ($R^2 = 0.9720$), as shown in Fig. S1.†

Table 2 Extraction yields of *C. longa* constituents by HDES-based microemulsions ($n = 3$, mean ± SEM)

	Extraction yields (wt%, dry basis)			
Microemulsion	Bis	Dem	Cur	*ar*-Tur
HDES of octanoic acid : menthol (70 : 30, mass ratio)				
ME-71	0.79 ± 0.01	1.71 ± 0.01	4.03 ± 0.02	0.64 ± 0.02
ME-72	0.95 ± 0.03	2.00 ± 0.05	4.56 ± 0.09	0.72 ± 0.02
ME-73	0.40 ± 0.00	1.00 ± 0.01	2.21 ± 0.03	0.29 ± 0.00
ME-74	1.32 ± 0.01	2.56 ± 0.01	6.15 ± 0.02	1.11 ± 0.01
ME-75	0.52 ± 0.00	1.19 ± 0.00	2.71 ± 0.00	0.41 ± 0.00
ME-76	1.22 ± 0.01	2.38 ± 0.01	5.70 ± 0.01	1.03 ± 0.01
ME-77	1.03 ± 0.00	2.03 ± 0.00	4.79 ± 0.01	0.87 ± 0.01
ME-78	0.61 ± 0.00	1.30 ± 0.00	2.98 ± 0.00	0.54 ± 0.00
HDES of octanoic acid : menthol (40 : 60, mass ratio)				
ME-41	2.09 ± 0.01	3.82 ± 0.02	8.99 ± 0.02	1.71 ± 0.01
ME-42	1.07 ± 0.00	2.11 ± 0.01	4.89 ± 0.01	0.81 ± 0.01
ME-43	2.04 ± 0.00	3.80 ± 0.01	9.07 ± 0.00	1.66 ± 0.01
ME-44	1.62 ± 0.01	3.06 ± 0.01	7.28 ± 0.01	1.36 ± 0.01
ME-45	0.94 ± 0.01	1.84 ± 0.03	4.29 ± 0.08	0.74 ± 0.01
ME-46	1.11 ± 0.00	2.19 ± 0.00	5.10 ± 0.02	0.95 ± 0.01
ME-47	0.85 ± 0.00	1.77 ± 0.01	4.11 ± 0.00	0.68 ± 0.00
HDES of octanoic acid : menthol (20 : 80, mass ratio)				
ME-21	1.59 ± 0.00	3.00 ± 0.00	6.93 ± 0.01	1.35 ± 0.01
ME-22	1.31 ± 0.01	2.53 ± 0.00	5.87 ± 0.01	1.02 ± 0.01
ME-23	1.69 ± 0.06	3.04 ± 0.01	7.36 ± 0.20	1.39 ± 0.01
ME-24	1.57 ± 0.01	2.97 ± 0.01	6.92 ± 0.07	1.45 ± 0.01
ME-25	1.90 ± 0.00	4.16 ± 0.01	8.10 ± 0.05	1.50 ± 0.00

Curs are challenging to extract because of their high lipophilicity, limiting their delivery.[26] Hydrophilic DES containing choline chloride and glycerol[27] and Cur–ibuprofen eutectics[28] have been documented to improve the solubility and dissolution of Cur when compared to raw Cur. DES-based surfactant-free microemulsions enhanced the solubilisation and extraction of Cur from CL (choline chloride + lactic acid, 1 : 1), resulting in a twofold increase in Cur solubility and an excellent extraction yield of 90%.[29] The DES-based surfactant-free ME had CL extraction yields of 1.180, 0.273, and 0.326 wt% for Cur, Dem, and Bis, respectively,[29] while the surfactant-free ME without DES resulted in extraction yields of 0.921, 0.318, and 0.289, respectively[30] (Table 3). In addition, the extraction yields by ME-21, ME-23 – ME-25, ME-41, ME-43 – ME-44 were higher than those by Soxhlet extraction with methanol, ultrasonicate- and microwave-assisted extraction with acetone and ethanol[31,32] (Table 3). It also suggests that HDES could produce ME with the high solubility of CL chemicals. Thus, HDES-based MEs are effectively alternative solvents for Curs extraction.

NO inhibitory effects of HDES-based MEs in LPS-activated murine macrophages

DESs are eutectic mixtures of ionised species with unique ionic solvent properties that help improve the therapeutic efficacy of standard anti-cancer drugs[33] and antibiotics.[34] DESs with menthol and saturated fatty acids of different chain lengths have been shown to have pharmacological benefits, such as wound healing and antibacterial properties.[18] The MEs are suitable for the simultaneous extraction of Cur and *ar*-Tur, in which turmeric oil enhances the anti-inflammatory properties of Cur.[35] We investigated the anti-inflammatory effects of ME-based CL extracts in LPS-activated RAW264.7 macrophages. All ME-based CL extracts were diluted with the culture medium before being added directly to the cells. Cell viability was greater than 80% for all ME-based CL extract treatments, with Cur concentrations ranging from 31.3 to 500 nM and the corresponding MEs. These non-toxic doses of ME-based CL extract with the specified Cur concentration and blank MEs were employed to determine NO inhibitory activity. In the same manner as the ME-based CL extract, blank MEs were diluted, and their concentration in the culture medium was expressed as a %v/v. The ME-24 formulation inhibited NO production the most ($IC_{50} = 0.00833 \pm 0.00120$%v/v), followed by ME-23 ($IC_{50} = 0.0136 \pm 0.0023$%v/v), and ME-71 ($IC_{50} = 0.0219 \pm 0.0041$%v/v) (Table 4). Four MEs with IC_{50} values less than 200 nM Cur exerted the highest NO-inhibiting activity among the ME-based CL extracts studied (Table 4 and Fig. S2–S4†). Based on the Cur concentration, the ME-23-based CL extract (IC_{50} value = 75.2 ± 6.7 nM) inhibited NO secretion the most, followed by ME-43-, ME-22-, and ME-24-based CL

Table 3 The extraction efficiency of curcuminoids from *C. longa* using different solvents and extraction methods[a]

		Extraction yields (wt%, dry basis)		
Extraction methods	Solvents	Bis	Dem	Cur
Stirring[29]	NADES-based microemulsions [NADES (choline chloride : lactic acid)/ ethanol/triacetin, 35/27.5/37.5]	0.326	0.273	1.180
Stirring[30]	Surfactant-free microemulsion [triacetin/ethanol/water, 36/24/40]	0.289	0.318	0.921
	Ethanol	0.092	0.134	0.434
Soxhlet extraction[31]	Methanol	0.53	0.71	1.87
Ultrasonicate-assisted extraction[32]	Acetone	—	—	4.000
	Ethanol	—	—	3.285
Microwave-assisted extraction[32]	Acetone	—	—	6.857
	Ethanol	—	—	4.857

[a] NADES, Natural Deep Eutectic Solvents.

Table 4 NO inhibitory activity of curcumin in microemulsion-based *C. longa* extracts ($n = 9$, mean ± SEM)

Microemulsion	IC_{50} of Cur (nM) in the CL extract of HDESs-based MEs	IC_{50} of HDESs-based MEs (%v/v)
HDES of octanoic acid : menthol (70 : 30, mass ratio)		
ME-71	400 ± 90	0.0219 ± 0.0041
ME-72	270 ± 82	> 0.0371
ME-73	400 ± 67	> 0.0371
ME-74	300 ± 23	0.0277 ± 0.0051
HDES of octanoic acid : menthol (40 : 60, mass ratio)		
ME-41	360 ± 32	0.0268 ± 0.0036
ME-42	230 ± 30	0.0222 ± 0.0023
ME-43	126 ± 1	0.0326 ± 0.0076
ME-44	216 ± 1	0.0260 ± 0.0031
HDES of octanoic acid : menthol (20 : 80, mass ratio)		
ME-21	> 500	> 0.0371
ME-22	137 ± 1	0.0256 ± 0.0028
ME-23	75.2 ± 6.7	0.0136 ± 0.0023
ME-24	157 ± 4	0.00833 ± 0.00120
ME-25	220 ± 48	0.0288 ± 0.0055

extracts ($IC_{50} = 126 \pm 1$, 137 ± 1, and 157 ± 4 nM, respectively). The ME-based CL extract containing OA : menthol (70 : 30, mass ratio) HDES inhibited NO with IC_{50} values between 270 and 400 nM. Dimethyl sulfoxide (DMSO)-, methanol-, and ethanol-based CL extracts, as well as authentic Cur dissolved in DMSO, minimally inhibited NO secretion, with IC_{50} >500 nM (Fig. S5†). Therefore, the ME-23-based CL extract was chosen for further studies on its anti-inflammatory activity, cellular delivery, and stability.

NO inhibitory effect of ME-23-based CL extract in LPS-activated murine macrophages

The inhibition of NO secretion by Cur and Curs dissolved in ME-23 was compared to that of the CL extract produced with ME-23. In addition, the components of blank ME-23, including menthol and OA, were examined and compared to their equivalent ME. The NO inhibitory activity was determined using non-toxic doses of Cur, OA, and menthol (Fig. S6†). Cur and Curs

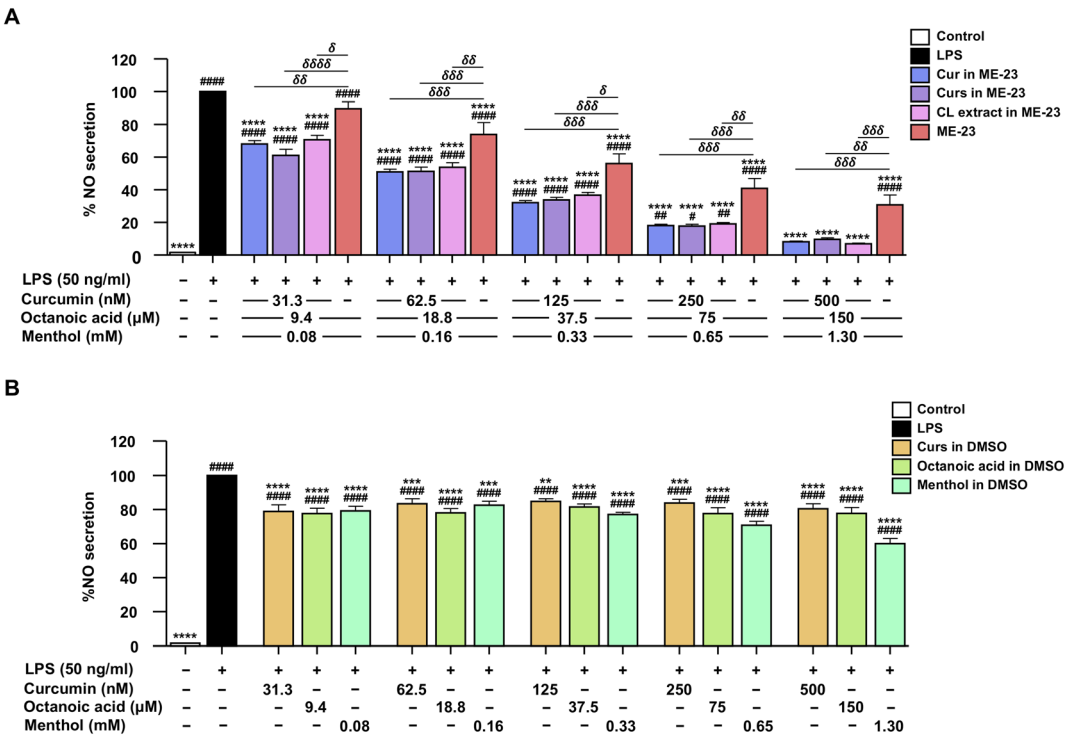

Fig. 2 NO inhibition in LPS-activated murine macrophages by Cur in ME-23, Curs in ME-23, CL extract in ME-23, and ME-23 (A) and Curs, octanoic acid, and menthol in DMSO (B). Data are presented as mean ± SEM of three independent experiments in triplicate. #p <0.05, ##p <0.01, and ####p <0.0001 *vs.* untreated control; **p <0.01, ***p <0.001, ****p <0.0001 *vs.* LPS-stimulated cells; δp <0.05, $\delta\delta$p <0.01, $\delta\delta\delta$p <0.001, and $\delta\delta\delta\delta$p <0.0001 *vs.* ME-23.

dissolved in ME-23, and ME-23-based CL extract significantly inhibited NO secretion to the same extent, which is better than the corresponding blank ME-23 (Fig. 2A). Cur dissolved in DMSO at nanomolar concentrations did not inhibit NO production (Fig. S5D†). Cur dissolved in ME-23 ($IC_{50} = 64.8 \pm 3.7$ nM) inhibited NO secretion ~103 times more effectively than Cur in DMSO, which had an IC_{50} in the micromolar range ($IC_{50} = 6.7 \pm 0.6$ μM) (Fig. 2A and S7†). OA and menthol dissolved in DMSO at the same concentrations as ME-23 reduced NO levels, and menthol was more effective than OA. However, their NO inhibition effects were lower than that of ME-23. These findings suggest that ME-23 may deliver CL constituents into cells, resulting in NO inhibition. OA and menthol in ME-23 are also NO-inhibiting components. Our findings align with the notion that HDES components (OA and menthol) have anti-inflammatory effects in activated macrophages, and their potency improves with the ME system.

Effect of ME-23-based CL extract on the production of inflammatory cytokines in LPS-activated murine and differentiated human macrophages

Cur (500 nM) was prepared in the form of authentic Cur in ME-23, Curs in ME-23, ME-23-based CL extract, and Cur in DMSO, and their effects on the production of TNF-α, IL-6, and IL-1β in LPS-stimulated RAW264.7 cells were evaluated. The effects of OA and menthol were also explored. After stimulation with LPS, the levels of TNF-α (Fig. 3A), IL-6 (Fig. 3B), and IL-1β (Fig. 3C) were markedly increased compared with the control without any treatment. Interestingly, treatment of the cells with Cur in ME-23, Curs in ME-23, and ME-23-based CL extract significantly reduced all inflammatory cytokines compared with LPS-treated cells. Furthermore, Cur and Curs, in combination with ME-23 tended to lower TNF-α and IL-1β levels more than ME-23 treatment alone. Menthol dissolved in DMSO considerably inhibited the release of TNF-α and IL-1β, whereas OA did not affect inflammatory cytokine secretion.

In addition, differentiated THP-1 macrophages stimulated by LPS were used as another model cell of inflammation. Consistent with LPS-activated murine macrophages, a non-toxic dose of Cur (500 nM) in different preparations (Cur in ME-23, Curs in ME-23, and ME-23-based CL extract) dramatically reduced TNF-α and IL-6 (Fig. S8A–C†). ME-23 treatment alone decreased IL-6 levels significantly but tended to reduce TNF-α levels. These findings show that ME-23 and its CL extract have anti-inflammatory properties by lowering the production of pro-inflammatory cytokines in two inflammatory model immune cells. The HDES-based ME-23 serves as a THDES, which provides beneficial anti-inflammatory effects and carries CL constituents.

The bioavailability of Cur is poor in humans, limiting its use.[36] Cur-microemulsion has been shown to improve relative bioavailability 22.6-fold more than a Cur suspension.[14] Comparing Cur in aqueous solutions to that in SMEDDS, rat pharmacokinetics revealed a 10- to 14-fold improvement in Cur absorption.[23] The relative bioavailability of daidzein in the form of borneol/menthol eutectic mixes was less than that of its microemulsion, with 1.5 times and 3.65 times higher

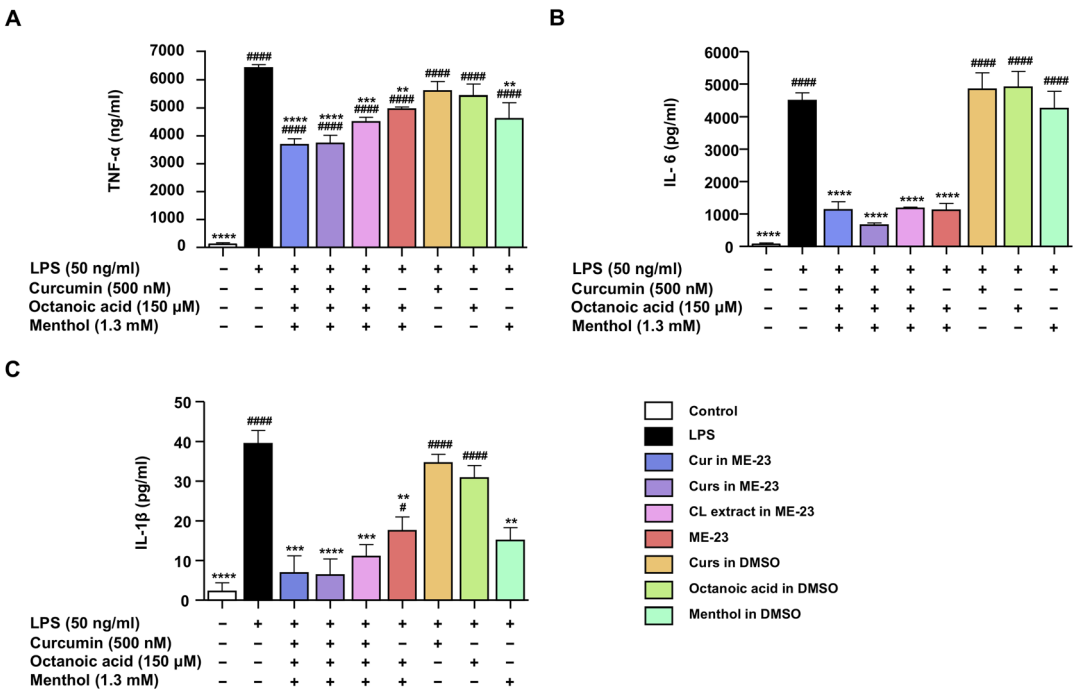

Fig. 3 Anti-inflammatory effects of Cur in ME-23, Curs in ME-23, CL extract in ME-23, and ME-23, as well as Curs, octanoic acid, and menthol in DMSO against inflammatory cytokines TNF-α (A), IL-6 (B), and IL-1β (C) production in LPS-activated murine macrophages. Data are presented as mean ± SEM of three independent experiments. #p <0.05, ####p <0.0001 *vs.* untreated control; **p <0.01, ***p <0.001, ****p <0.0001 *vs.* LPS-stimulated cells.

bioavailability, respectively, when compared to a daidzein suspension.[25] As Cur has been effective in clinical trials of inflammation-mediated diseases, preclinical studies of Cur in HDES-based ME-23 should be conducted in animal experiments to ensure its effectiveness, safety, and bioavailability to facilitate pharmaceutical applications of our findings.

Cellular uptake of ME-23-based CL extract in LPS-activated murine macrophages

A non-toxic dose of Cur at the nanomolar range (500 nM) from the two preparations (Cur in ME-23 and ME-23-based CL extract) was detected as a green autofluorescent signal within LPS-activated murine macrophages following a 12 h incubation by 3D-Holotomography (Fig. 4A) and confocal microscopy analysis (Fig. 4B), indicating the delivery of Cur within the macrophages by ME-23. As a positive control, both methods showed that the micromolar concentrations of Cur in DMSO (10 and 20 μM) resulted in a more significant accumulation of Cur in macrophages. These findings indicate that Cur in the two preparations (ME-23 and ME-23-based CL extract) was successfully delivered into macrophages. Even though numerous studies reveal a significant intensity of green fluorescence of Cur in cells when treated with micromolar range concentrations,[37,38] the less accumulation of green fluorescence intensity of Cur observed in our cell model could be attributed to the use of nanomolar range Cur concentrations in treating cells.

Stability of CL chemicals in HDES and HDES-based microemulsion

This experiment aimed to evaluate the stability profiles of Curs and *ar*-Tur in OA : menthol (20 : 80 mass ratio) and ME-23. Based on HDES utilizing a 20 : 80 mass ratio of OA : menthol, the initial solution of the CL extract comprised Bis (0.334 ± 0.002 mg mL^{-1}), Dem (0.230 ± 0.002 mg mL^{-1}), Cur (0.652 ± 0.003 mg mL^{-1}), and *ar*-Tur (0.496 ± 0.005 mg mL^{-1}). The ME-23-based CL extracts included Bis (0.226 ± 0.001 mg mL^{-1}), Dem (0.163 ± 0.002 mg mL^{-1}), Cur (0.513 ± 0.006 mg mL^{-1}), and *ar*-Tur (0.311 ± 0.017 mg mL^{-1}). Longer periods and greater temperatures enhance the degradation processes when maintained at varying temperatures (Fig. 5). The stability characteristics of the target compounds were the same manner as those when they were stored in HDES and ME-23. Bis (Fig. 5A and B) and Cur (Fig. 5E and F) deteriorated gradually with lengthy

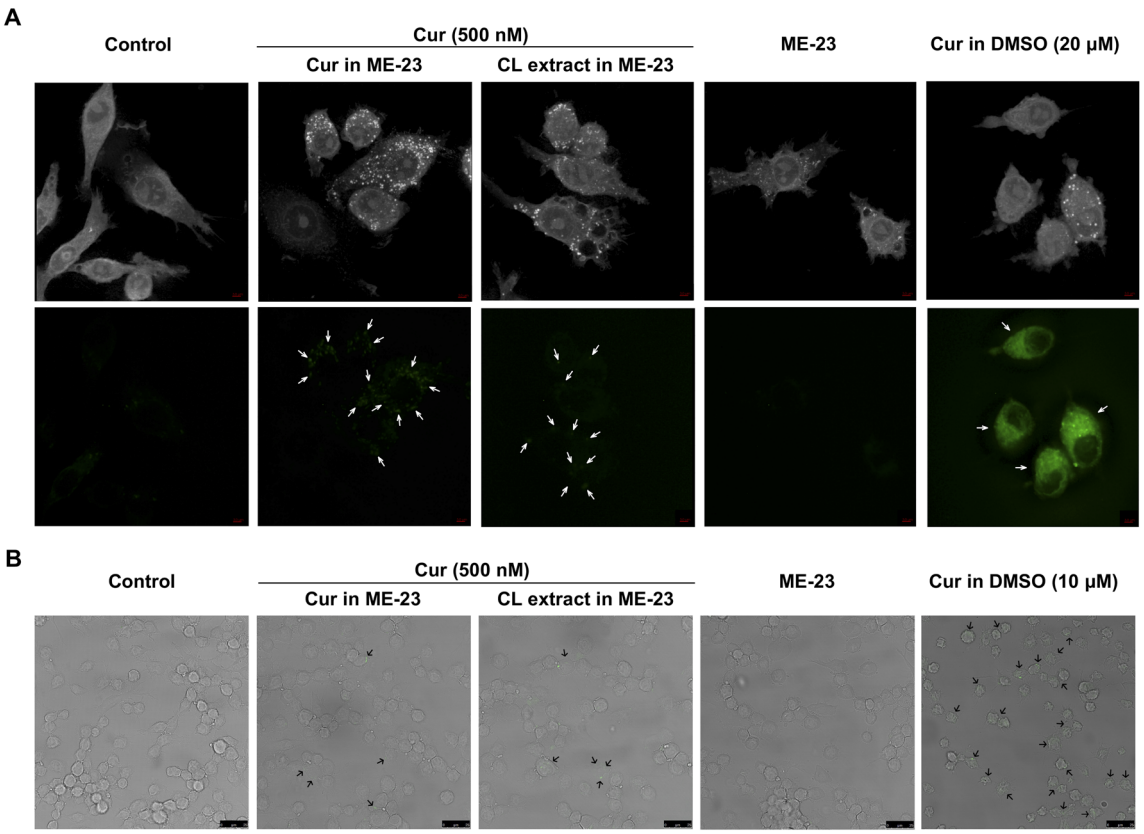

Fig. 4 Cellular uptake of Cur in ME-23 and Cur in ME-23-based CL extract in LPS-activated murine macrophages. Cur (green fluorescence) was detected in LPS-activated macrophages treated with Cur in ME-23 (500 nM), Cur in ME-23-based CL extract (500 nM), and Cur in DMSO (10 and 20 μM). The representative maximum intensity projection images (upper panel) and fluorescence images (lower panel) were acquired by 3D-Holotomographic Microscopy (scale bar, 3 μm) (A). The representative confocal laser scanning microscopy images were acquired by Confocal Laser Scanning Microscope (scale bar, 25 μm) (B). The cellular uptake of Cur in macrophages is indicated by white and black arrows.

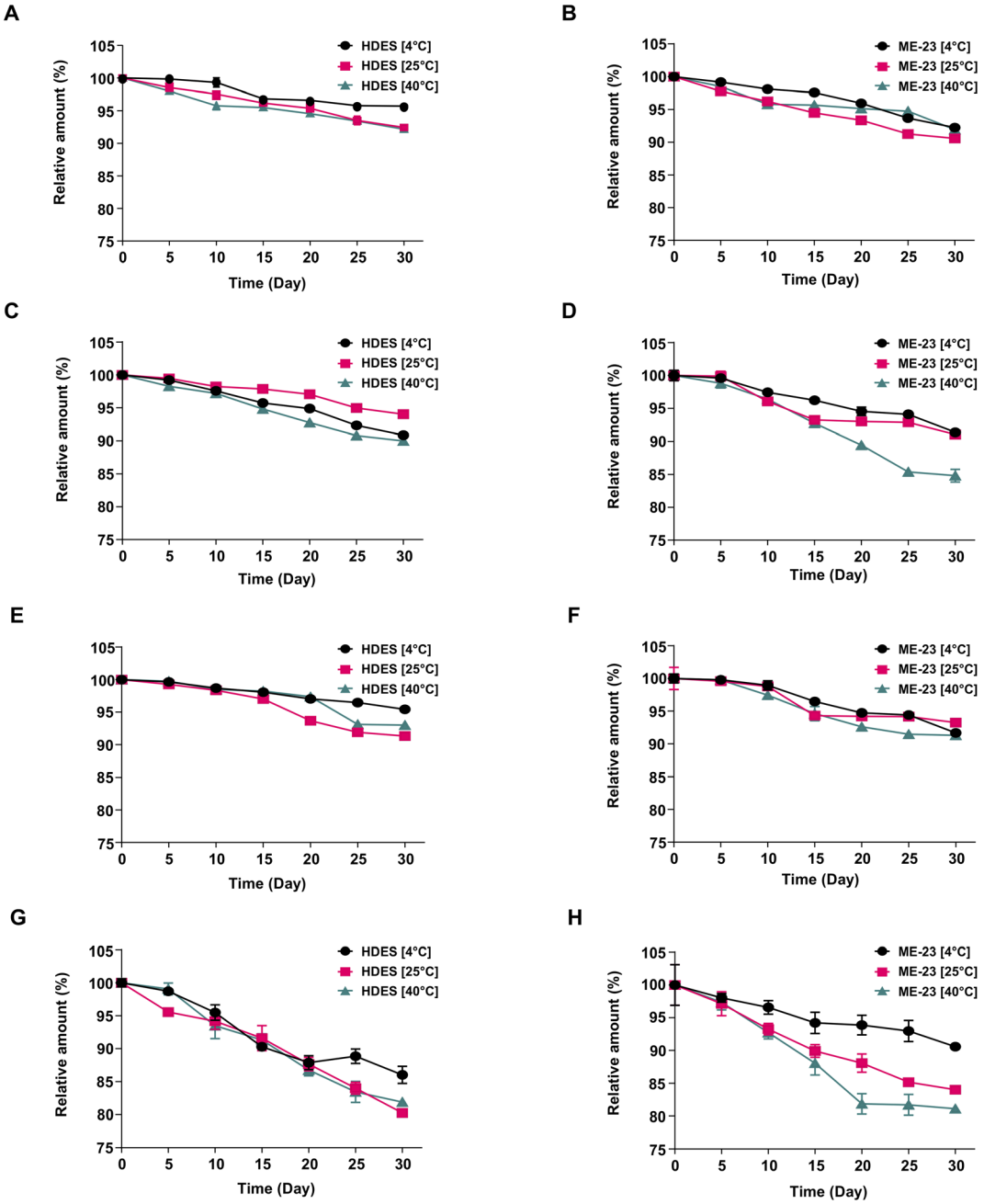

Fig. 5 Stability of Bis (A), Dem (C), Cur (E), and *ar*-Tur (G) in HDES (OA : menthol, 20 : 80 mass ratio) and those Bis (B), Dem (D), Cur (F), and *ar*-Tur (H) in ME-23 after 30 day storage at various temperatures. Data are presented as mean ± SEM of three independent experiments.

storage, although more than 90% remained after being kept in HDES and ME-23. At 40 °C, the degradation of Dem in ME-23 (84.8% remaining) was substantially faster than in HDES, where 90% of Dem remained (Fig. 5C and D). Compared to Curs, *ar*-Tur was relatively susceptible to degradation (Fig. 5G and H). After storage, the above 90% remaining of *ar*-Tur was noticed in ME-23 at 4 °C, and *ar*-Tur stability was greater than that of HDES (Fig. 5H).

Cur was highly unstable to chemical degradation and tended to crystallise in aqueous acidic solutions.[39] Cur stability was improved in camphor-menthol DES[40] and a microemulsion made with the non-ionic surfactant Triton X-100 and a DES [tetra-*n*-butylammonium chloride (TBAC) and *n*-decanoic acid (DA) in a 1 : 2 molar ratio].[41] Tetra-*n*-butylammonium chloride is a health hazard that cannot be used in food or pharmaceuticals. After 15 days, Cur in the water-in-TBAC : DA microemulsions had degraded by 20–25%.[41] After 30 days, 90% of Cur was stable in the HDES-based ME-23. The stability profiles of Curs and *ar*-Tur in HDES did not differ significantly from those of HDES-based ME. Therefore, although the HDES-based system contains water, Cur should be protected by an HDES compartment. Further investigation of the acid-base stabilisation of Cur by HDES-based ME is recommended.

Experimental

Materials

Dem (≥98%) and Cur (≥99.5%) were purchased from Sigma-Aldrich (St. Louis, MO, USA). Bis (≥98%), OA (≥98%), and L-menthol (>99.0%) were purchased from Tokyo Chemical Industry Co., Ltd. (Tokyo, Japan). *ar*-Tur (≥90%) was supplied by Toronto Research Chemicals Inc. (ON, Canada). The reference Curs were obtained from Acros Organics™ (Thermo Fisher Scientific Inc., NJ, USA) and contained Cur (73.5 wt%), Dem (27.3 wt%), and Bis (0.136 wt%). Rhizomes of CL were collected from a market in Nakhon Si Thammarat (Thailand). The sample was cut and dried in an oven for two days at 50 °C. CL was pulverised and sieved (0.5 mm) before being used in subsequent experiments.

Preparation of HDES-based microemulsion

Based on earlier research, a HDES containing menthol and octanoic acid was synthesised.[18] The HDES was prepared using OA : menthol mass ratios of 20 : 80, 40 : 60, and 70 : 30, which correspond to molar ratios of 1 : 3.6, 1 : 1.4, and 2.5 : 1, respectively. DESs were initiated by stirring and heating at 70 °C for 20 min, while the components were continuously mixed. The mass ratios of the components were selected based on their capacity to dissolve the Curs and *ar*-Tur. As in the previous investigation, the ME system of HDES (20 : 80 mass ratio of OA : menthol) as the oil phase and Tween 80 : PG as a surfactant mixture were created.[42] Similarly, pseudo-ternary phase diagrams were produced with HDES (40 : 60 and 70 : 30 mass ratios of OA : menthol) as the oil phase. Tween 80 : PG (1 : 1) surfactant mixtures were also studied. The HDES was then mixed with the surfactant mixture in the following weight ratios: 10 : 0, 9 : 1, 8 : 2, 7 : 3, 6 : 4, 5 : 5, 4 : 6, 3 : 7, 2 : 8, 1 : 9, and 0 : 10. Each mixture was homogenised before water was added in a dropwise manner. The liquid was vigorously stirred to achieve homogeneity during this procedure before being placed on a dark background and illuminated with white light. When the samples emerged as transparent liquids, they were designated MEs. The CHEMIX School program was used to identify ME zones (Arne Standards, Bergen, Norway).

Photon correlation spectroscopy to analyse the microemulsion droplet size

Photon correlation spectroscopy in conjunction with dynamic light scattering (Zeta potential analyser, Model Zeta Nano ZS ZEN 3600, Brookhaven, USA) was used to measure the droplet sizes of the HDES-based MEs and the associated CL extracts.[23] Prior to analysis, each ME-based CL extract was diluted 1000-fold with the corresponding blank ME to reduce color interference. In the instrument software, viscosity (0.89 cP) and refractive index (1.330) of water were inputted. Measurements were made at 25 °C using light scattering at a 90-degree angle. Three independent analyses were conducted for each sample. In addition, the MEs were diluted (1/1000) in water before droplet size analysis. The procedure was performed to guarantee the particle size after dilution during cell-based testing.

Extraction efficiency of curcuminoids and *ar*-Tur utilising a microemulsion based on HDES

Microemulsions containing HDES were evaluated as solvents to extract Curs and *ar*-Tur from CL. Numerous ME formulations were designed according to the pseudo-ternary phase diagrams (Fig. 1), as listed in Table 1. In these tests, 50 mg of dried CL rhizome was extracted with 1 mL of HDES-based ME using 37 kHz ultrasonication for 60 min. The extracts were collected at a centrifugation rate of 7155×*g*. The extraction yields of Bis, Dem, Cur, and *ar*-Tur were determined using high-pressure liquid chromatography with a UV detector (Thermo Fisher, Waltham, MA, USA). The HPLC protocol was based on a previous report.[42]

Cell culture

The RAW264.7 cell line was acquired from the American Type Culture Collection (Manassas, VA, USA). Human THP-1 monocytes was purchases from the Cell Lines Service (Eppelheim, Baden-Württemberg, Germany). These two cell lines were cultured in RPMI-1640 supplemented with 10%v/v endotoxin-free fetal bovine serum (Biochrom GmbH, Berlin, Germany), penicillin/streptomycin (100 U mL^{-1}), and 2 mM glutamine (Gibco, Gaithersburg, MD, USA). The cells were maintained at 37 °C in a humidified atmosphere containing 5% CO_2.

Cytotoxicity test

Cytotoxicity was assessed using the 3-(4,5-dimethylthiazol-2-yl)-2,5-diphenyltetrazolium bromide (MTT) reagent (Sigma-Aldrich) in LPS-activated RAW264.7 and differentiated human THP-1 macrophages. To differentiate THP-1 monocytes into macrophages, cells were exposed to 100 nM phorbol 12-myristate 13-acetate (PMA) (Sigma-Aldrich) for 48 h. The differentiated THP-1 cells were then incubated in RPMI-1640 without PMA for 24 h. RAW264.7 macrophages and differentiated human THP-1 macrophages (3.1×10^5 cells per cm^2) were seeded into 96-well plates and pre-treated for 1 h with sample solutions. The samples were MEs based on the HDES and CL extracts at varying concentrations. HPLC was used to quantify the Bis, Dem, Cur, and *ar*-Tur concentrations in the CL extracts before performing the experiments. In addition, CL extracts produced using organic solvents were subjected to their cytotoxicity. ME-23 was chosen as the best HDES-based ME for delivering the CL extracts. Cur and Curs were prepared using ME-23, and their cytotoxicities were compared to Curs prepared in DMSO. Individual components, such as OA, menthol, and HDES (OA : menthol, 20 : 80 mass ratio), were tested and compared with the blank ME-23. After 1 h of pretreatment with the indicated samples, 50 ng mL^{-1} LPS (*Escherichia coli* 0111:B4, Sigma-Aldrich) was added and the incubation was extended for 24 h. The culture medium was removed, and cells were then incubated for 3 h at 37 °C with 100 μL of MTT solution (0.5 mg mL^{-1}). Each well was dissolved in 200 μL of DMSO after discarding the solution, and the absorbance was measured at 560 nm using a microplate reader (Thermo Fisher Scientific).

Griess assay

The Griess reagent[43] was used to determine nitrite levels, a stable end-product of NO synthesis. RAW264.7 cells (3.1×10^5 cells per cm^2) were seeded into 96-well plates for 24 h. Then, the cells were pre-treated for 1 h with various concentrations of samples, providing cell viability of over 80%. The samples used were the same as those used in the cytotoxicity tests. LPS (50 ng mL^{-1}) was added and the cells were incubated for 24 h. The culture medium was collected and subjected to the Griess reagent. Absorbance was measured at 540 nm using a microplate reader (Thermo Fisher Scientific). The nitrite concentration was calculated from the sodium nitrite standard curve. The half-maximal inhibitory concentration of NO (IC_{50}) was derived using non-linear regression in GraphPad Prism version 9.1.1 from a dose–response curve (GraphPad Software, San Diego, CA, USA).

Enzyme-linked immunosorbent assay

RAW264.7 cells and differentiated human THP-1 macrophages were seeded into 96-well plates at a density of 3.1×10^5 cells per cm^2. The cells were pre-treated with ME-23, OA, menthol, and 500 nM Cur from different preparations (Cur in ME-23, Curs in ME-23, CL extract in ME-23, and Cur in DMSO), before being stimulated with 50 ng mL^{-1} LPS for 24 h. Culture supernatants were collected, and the levels of inflammatory cytokines (TNF-α, IL-6, and IL-1β) were determined according to the manufacturer's instructions (BioLegend, San Diego, CA, USA).

In vitro cellular uptake

RAW264.7 cells at a density of 7×10^4 cells per cm^2 were seeded on TomoDish (Tomocube, Inc., Daejeon, Republic of Korea) for 24 h. Cells were pre-treated for 1 h with ME-23, 500 nM Cur from the two different preparations (Cur in ME-23 and CL extract in ME-23), and Cur in DMSO (10 μM), followed by LPS (50 ng mL^{-1}) treatment for 12 h. TomoDish-containing cells were directly examined using 3D-Holotomographic Microscopy (HT-2H, Tomocube, Inc). The visualisation of the maximum intensity projection images and green fluorescence signal of Cur at an excitation/emission wavelength of 488/530 nm was carried out using TomoStudio™, Tomocube, Inc.

Another set of cells with a density of 2.4×10^5 cells per cm^2 were seeded on coverslips on 24-well plates for 24 h. Then the cells were washed three times with ice-cold PBS and fixed with 4% paraformaldehyde for 30 min at 25 °C. The coverslips were placed on microscope slides, and the green autofluorescence signal of Cur was acquired using a Leica TCS SP5 II confocal laser scanning microscope (Leica Microsystems, Wetzlar, Germany).

Thermal stability evaluation of Curs and *ar*-Tur in HDES and HDES-based microemulsion

In this study, the thermal stabilities of Curs and *ar*-Tur were evaluated based on previous studies.[44] CL extracts were generated using HDES (OA : menthol, 20 : 80 mass ratio), and the ME (ME-23) consisted of HDES/Tween 80 : propylene glycol (1 : 1)/water (25/70/5). The sample solutions were kept in the dark at 4, 25, or 40 °C. After 5, 10, 15, 20, 25, and 30 days, the concentrations of the target constituents in the different samples ($n = 3$) were measured using HPLC.

Statistical analysis

The mean ± standard error of the mean (SEM) of three independent experiments was used to express all experimental data. GraphPad Prism version 9.1.1 (GraphPad Software) was used to determine any statistical differences between the treatment groups using one-way ANOVA followed by Dunnett's multiple comparison test. Values of $p < 0.05$ were considered statistically significant.

Conclusions

This study proposes a novel HDES-based ME for CL extraction with a high extraction yield, carriers for Cur delivery, and improved anti-inflammatory efficacy. Interestingly, Curs, present in ME-23-based CL extraction, suppressed NO release and reduced inflammatory cytokines in LPS-activated murine and differentiated human macrophages more effectively than Curs dissolved in DMSO. Authentic Cur in ME-23 inhibited NO production more than 103 times greater than Cur in the conventional solvent. HDES-based ME-23 is capable of delivering Cur into the murine macrophages. The stability profile of Cur was over 90% after storage for 30 days in HDES and HDES-based ME. ME-23 is a promising CL extraction reagent that possesses anti-inflammatory activity while being environmentally friendly, making it suitable for applications in the pharmaceutical and cosmetic industries. Animal models must be used to determine the anti-inflammatory activity, safety, and bioavailability of ME-23-based CL extract prior to its widespread use.

Author contributions

Nassareen Supaweera: Methodology, formal analysis, investigation, data curation, writing – original draft. Wanatsanan Chulrik and Chutima Jansakun: Investigation, validation. Phuangthip Bhoopong: Visualization, resources. Gorawit Yusakul and Warangkana Chunglok: Conceptualisation, methodology, resources, writing - review and editing, supervision, funding acquisition.

Conflicts of interest

The authors declare no competing financial interest.

Acknowledgements

This research work was funded by the Thailand Science Research and Innovation Fund (Contract No WU-FF64102) and the new strategic research (P2P) project, Walailak University, Nakhon Si Thammarat, Thailand. N. Supaweera was supported by Walailak University PhD Scholarships for High Potential Candidates to Enroll in Doctoral Programs (Contract No HP011/2021). We acknowledge Mr Shin Dongjun (Tomocube, Inc., Daejeon, Republic of Korea), Miss Bongkotchakorn

Peereeyaphat, and Miss Yabeela Samun (Hollywood International Ltd., Thailand) for their technical assistance with cell imaging.

References

1 J. Sharifi-Rad, Y. E. Rayess, A. A. Rizk, C. Sadaka, R. Zgheib, W. Zam, S. Sestito, S. Rapposelli, K. Neffe-Skocińska, D. Zielińska, B. Salehi, W. N. Setzer, N. S. Dosoky, Y. Taheri, M. El Beyrouthy, M. Martorell, E. A. Ostrander, H. A. R. Suleria, W. C. Cho, A. Maroyi and N. Martins, *Front. Pharmacol.*, 2020, **11**, 01021.

2 CBI, The European market potential for curcuma longa (turmeric), 2022, **https://www.cbi.eu/market-information/spices-herbs/curcuma/market-potential**, accessed on April 23, 2022.

3 M.-T. Huang, W. Ma, Y.-P. Lu, R. L. Chang, C. Fisher, P. S. Manchand, H. L. Newmark, A. H. Conney and M. You, *Carcinogenesis*, 1995, **16**, 2493–2497.

4 J. W. Daily, M. Yang and S. Park, *J. Med. Food*, 2016, **19**, 717–729.

5 Y. Huang, S. Cao, Q. Zhang, H. Zhang, Y. Fan, F. Qiu and N. Kang, *Arch. Biochem. Biophys.*, 2018, **646**, 31–37.

6 J.-C. Wu, M.-L. Tsai, C.-S. Lai, Y.-J. Wang, C.-T. Ho and M.-H. Pan, *Food Funct.*, 2014, **5**, 12–17.

7 A.-F. Hsiao, Y.-C. Lien, I. S. Tzeng, C.-T. Liu, S.-H. Chou and Y.-S. Horng, *Compl. Ther. Med.*, 2021, **63**, 102775.

8 L. T. Marton, L. M. Pescinini-E-Salzedas, M. E. C. Camargo, S. M. Barbalho, J. F. D. S. Haber, R. V. Sinatora, C. R. P. Detregiachi, R. J. S. Girio, D. V. Buchaim and P. Cincotto Dos Santos Bueno, *Front. Endocrinol.*, 2021, **12**, 669448.

9 K. B. Megha, X. Joseph, V. Akhil and P. V. Mohanan, *Phytomedicine*, 2021, **91**, 153712.

10 A. Płóciennikowska, A. Hromada-Judycka, J. Dembińska, P. Roszczenko, A. Ciesielska and K. Kwiatkowska, *J. Leukocyte Biol.*, 2016, **100**, 1363–1373.

11 R. Sawoo, R. Dey, R. Ghosh and B. Bishayi, *Immunol. Res.*, 2021, **69**, 334–351.

12 S. Kany, J. T. Vollrath and B. Relja, *Int. J. Mol. Sci.*, 2019, **20**, 6008.

13 B. Salehi, Z. Stojanović-Radić, J. Matejić, M. Sharifi-Rad, N. V. Anil Kumar, N. Martins and J. Sharifi-Rad, *Eur. J. Med. Chem.*, 2019, **163**, 527–545.

14 L. Hu, Y. Jia, F. Niu, Z. Jia, X. Yang and K. Jiao, *J. Agric. Food Chem.*, 2012, **60**, 7137–7141.

15 C. Ban, M. Jo, Y. H. Park, J. H. Kim, J. Y. Han, K. W. Lee, D.-H. Kweon and Y. J. Choi, *Food Chem.*, 2020, **302**, 125328.

16 C. Schiborr, A. Kocher, D. Behnam, J. Jandasek, S. Toelstede and J. Frank, *Mol. Nutr. Food Res.*, 2014, **58**, 516–527.

17 C. Huang, X. Chen, C. Wei, H. Wang and H. Gao, *Front. Pharmacol.*, 2021, **12**, 794939.

18 J. M. Silva, C. V. Pereira, F. Mano, E. Silva, V. I. B. Castro, I. Sá-Nogueira, R. L. Reis, A. Paiva, A. A. Matias and A. R. C. Duarte, *ACS Appl. Bio Mater.*, 2019, **2**, 4346–4355.

19 A. L. Rozza, F. Meira de Faria, A. R. Souza Brito and C. H. Pellizzon, *PLoS One*, 2014, **9**, e86686.

20 H. Wang and F. Meng, *J. Mol. Model.*, 2017, **23**, 279.

21 A. Hoshimoto, Y. Suzuki, T. Katsuno, H. Nakajima and Y. Saito, *Br. J. Pharmacol.*, 2002, **136**, 280–286.

22 X. Zhang, C. Xue, Q. Xu, Y. Zhang, H. Li, F. Li, Y. Liu and C. Guo, *Nutr. Metab.*, 2019, **16**, 40.

23 S. Setthacheewakul, S. Mahattanadul, N. Phadoongsombut, W. Pichayakorn and R. Wiwattanapatapee, *Eur. J. Pharm. Biopharm.*, 2010, **76**, 475–485.

24 M. Danaei, M. Dehghankhold, S. Ataei, F. Hasanzadeh Davarani, R. Javanmard, A. Dokhani, S. Khorasani and M. R. Mozafari, *Pharmaceutics*, 2018, **10**, 57.

25 Q. Shen, X. Li, W. Li and X. Zhao, *AAPS PharmSciTech*, 2011, **12**, 1044–1049.

26 K. Suresh and A. Nangia, *CrystEngComm*, 2018, **20**, 3277–3296.

27 T. Jeliński, M. Przybyłek and P. Cysewski, *Pharm. Res.*, 2019, **36**, 116.

28 I. Sathisaran, J. M. Skieneh, S. Rohani and S. V. Dalvi, *J. Chem. Eng. Data*, 2018, **63**, 3652–3671.

29 V. Huber, L. Muller, P. Degot, D. Touraud and W. Kunz, *Food Chem.*, 2021, **355**, 129624.

30 P. Degot, V. Huber, E. Hofmann, M. Hahn, D. Touraud and W. Kunz, *Food Chem.*, 2021, 336.

31 Y.-J. Kim, H. J. Lee and Y. Shin, *J. Agric. Food Chem.*, 2013, **61**, 10911–10918.

32 P. S. Wakte, B. S. Sachin, A. A. Patil, D. M. Mohato, T. H. Band and D. B. Shinde, *Sep. Purif. Technol.*, 2011, **79**, 50–55.

33 C. V. Pereira, J. M. Silva, L. Rodrigues, R. L. Reis, A. Paiva, A. R. C. Duarte and A. Matias, *Sci. Rep.*, 2019, **9**, 14926.

34 S. N. Pedro, A. T. P. C. Gomes, P. Oskoei, H. Oliveira, A. Almeida, M. G. Freire, A. J. D. Silvestre and C. S. R. Freire, *Int. J. Pharm.*, 2022, **616**, 121566.

35 S. Toden, A. L. Theiss, X. Wang and A. Goel, *Sci. Rep.*, 2017, **7**, 814.

36 C. D. Lao, M. T. t. Ruffin, D. Normolle, D. D. Heath, S. I. Murray, J. M. Bailey, M. E. Boggs, J. Crowell, C. L. Rock and D. E. Brenner, *BMC Complementary Altern. Med.*, 2006, **6**, 10.

37 R. Farajzadeh, N. Zarghami, H. Serati-Nouri, Z. Momeni-Javid, T. Farajzadeh, S. Jalilzadeh-Tabrizi, S. Sadeghi-Soureh, N. Naseri and Y. Pilehvar-Soltanahmadi, *Artif. Cells, Nanomed., Biotechnol.*, 2018, **46**, 2013–2021.

38 P. He, B. Tang, Y. Li, Y. Zhang, X. Liu, X. Guo, D. Wang, P. She and C. Xiao, *Int. J. Nanomed.*, 2021, **16**, 5053–5064.

39 M. Kharat, Z. Du, G. Zhang and D. J. McClements, *J. Agric. Food Chem.*, 2017, **65**, 1525–1532.

40 T. Sekharan, R. Chandira, S. C. Rajesh, T. Shunmugaperumal, C. T. Vijayakumar and B. S. Venkateswarlu, *Res. J. Pharm. Technol.*, 2021, **14**, 6430–6436.

41 D. Dhingra, M. Bisht, B. Bhawna and S. Pandey, *J. Mol. Liq.*, 2021, **339**, 117037.

42 K. Kongpol, N. Sermkaew, F. Makkliang, S. Khongphan, L. Chuaboon, A. Sakdamas, S. Sakamoto, W. Putalun and G. Yusakul, *Food Chem.*, 2022, **396**, 133728.

43 S. Jie, X. Zhang, B. Mark and F. Harry, *Sensors*, 2003, **3**.

44 Y. Liu, J. Li, R. Fu, L. Zhang, D. Wang and S. Wang, *Ind. Crops Prod.*, 2019, **140**, 111620.